

# In Vitro Soil Pb Solubility in the Presence of Hydroxyapatite

PENGCHU ZHANG\* AND JAMES A. RYAN

National Risk Management Research Laboratory, U.S. EPA,  
5995 Center Hill Avenue, Cincinnati, Ohio 45224

JOHN YANG

Department of Geological Sciences, University of Missouri,  
Columbia, Missouri 65211

The transformation of lead (Pb) in contaminated soils to pyromorphite, by the addition of phosphate minerals, may be an economic in-situ immobilization strategy that results in a reduction of bioavailable Pb. To test this hypothesis, we conducted two sets of soil–solution experiments under constant (i.e., fixed) or dynamic (i.e., variable) pH conditions, as a function of time. In both sets of experiments, Pb-contaminated soil was reacted with synthetic hydroxyapatite in order to determine the transformation rate of soil Pb to pyromorphite and the soluble Pb level during the reaction period. In the constant pH system, the soluble Pb concentration decreased with the addition of apatite at pH 4 and above. However, the transformation was pH-dependent and incomplete at relatively high pH ( $\geq 6$ ). The solubility of cerussite ( $\text{PbCO}_3$ ), the major Pb mineral in this soil, still exhibited a strong influence on the solubility of soil Pb. In the dynamic pH experiments, which simulated gastric pH conditions (i.e., pH variation from 2 to 7 within 25 or 45 min), both cerussite and added apatite were dissolved at low pH values (pH 2 and pH 3), and chloropyromorphite was rapidly precipitated from dissolved Pb and  $\text{PO}_4$  when the suspension pH was increased. Complete transformation of soil Pb to chloropyromorphite occurred in the pH dynamic experiments within 25 min, indicating rapid reaction kinetics of the formation of chloropyromorphite. Chloropyromorphite solubility controls the soluble Pb concentration during the entire duration of the pH dynamic experiments. This study demonstrates the importance of considering specific site conditions, such as pH, when considering evaluation of soil Pb bioavailability and in-situ immobilization of Pb in Pb-contaminated soils using phosphate amendment. Furthermore, this study demonstrates that the kinetics of conversion of soil Pb to chloropyromorphite in the presence of apatite is fast enough to occur during ingestion and that gastric pH conditions would favor the formation of chloropyromorphite, thus rendering ingested soil Pb nonbioavailable.

## Introduction

Lead-contaminated soil has long been considered a primary source of Pb exposure for young children. Remediation

action is considered when the total soil Pb content exceeds 500–1000 mg  $\text{kg}^{-1}$ . In situ immobilization of soil Pb had attracted much attention for its potential advantage as a cost-effective and environmentally benign remediation strategy. One approach is to amend Pb-contaminated soil with either soluble phosphate salts or insoluble phosphate minerals such as apatite [ $\text{Ca}_5(\text{PO}_4)_3(\text{OH}, \text{F}, \text{Cl} \dots)$ ]. Chemically and biologically reactive Pb forms or “labile Pb” in a contaminated soil can be transformed into insoluble pyromorphite [ $\text{Pb}_5(\text{PO}_4)_3(\text{Cl}, \text{F}, \text{OH} \dots)$ ], a lead phosphate mineral that is stable under conditions likely to be encountered in the surface environment. Pyromorphite is generally several orders of magnitude less soluble than the analogous lead carbonates and lead sulfates. By forming pyromorphite, the bioavailability of the ingested soil Pb is expected to be reduced due to the low solubility of the pyromorphite mineral.

Reduction of Pb concentration in aqueous solution and Pb-contaminated soil solution by adding phosphate mineral, hydroxyapatite [ $\text{Ca}_5(\text{PO}_4)_3\text{OH}$ ] (1–4), and phosphate rocks has been reported (5). Furthermore, formation of pyromorphite in reactions of aqueous Pb and soil Pb with phosphate minerals have also been confirmed (2, 6–8). The predominant mechanism of pyromorphite formation involves dissolution of Pb-bearing solids and phosphate minerals and pyromorphite precipitation. The precipitation reaction is rapid, and the reaction rate appears limited by the dissolution of the Pb minerals or of the added phosphate. Accordingly, there has been speculation about reduction in Pb bioavailability when the contaminated soil is ingested with apatite, before complete conversion of the labile Pb into pyromorphite has occurred. To test this, an investigation of the reactions of soil Pb and phosphate under gastric conditions is needed.

Bioavailability/bioaccessibility of soil Pb is assumed to be associated with the solubility and dissolution rates of the soil Pb in the gastrointestinal tract (GI tract). Thus, the effects of GI tract physiological factors such as gastric pH level, gastric physiochemistry, ratios of solid to gastric solution, stomach content, and stomach emptying time on soil Pb solubility are all issues. Lead mineral composition, particle size, and degree of encapsulation have been shown to affect the dissolution rate of soil Pb in in-vitro bioavailability assessments (9–11). However, there has been no evaluation of changes in solid Pb species during ingestion.

Our purpose was to evaluate the effects of geochemical and physiological parameters on the soil Pb-bioavailability and the effects of phosphate amendment on soil Pb bioavailability. A Pb contaminated soil was reacted with a synthetic hydroxyapatite in a pH range characteristic of a gastrointestinal tract. One series of measurements were conducted in soil suspensions with constant pH (pH-constant) to determine the solubility and dissolution rate of soil Pb in the presence of apatite. Another two experiments were carried out in a soil–apatite system in which the pH was adjusted with time during the reaction (pH-dynamic) to evaluate (1) the effect of reaction kinetics on the soluble Pb concentration in the GI tract and (2) the formation of pyromorphite during the simulated digestion process.

## Materials and Methods

**Materials.** The soil used in this study was provided by Dr. S. Traina of The Ohio State University, who obtained it from a residential area in Oakland, CA. The major source of Pb contamination in this soil was from a paint spill. The mineralogical properties associated with the soil particle size can be found in the literature (8). The total Pb content in

\* To whom correspondence should be addressed at his present address: Sandia National Laboratories, MS 0750, Albuquerque, NM 87185; telephone: 505-844-2669; fax: 505-844-7354; e-mail: PZHANG@SANDIA.GOV.

the whole soil (particle size < 2 mm) was 37 026 mg kg<sup>-1</sup>, the soil fraction used in this study, <0.5 mm, has a Pb content of 34 592 (± 45) mg kg<sup>-1</sup>. The detectable lead mineral in this soil fraction was cerussite (PbCO<sub>3</sub>) (8).

The source of phosphate used in this study was a synthetic hydroxyapatite [Ca<sub>5</sub>(PO<sub>4</sub>)<sub>3</sub>OH] obtained from Bio-Rad. It had a specific surface area of 67.3 m<sup>2</sup> g<sup>-1</sup> (BET nitrogen absorption) and a P/Ca molar ratio of 1.62, which is close to the ideal ratio of 1.67.

To conduct the reaction of soil Pb and apatite, the soil was mixed with hydroxyapatite at 23, 35, and 70 mg of apatite/g of soil. The molar ratios of phosphate to lead (P/Pb) in the soil-apatite mixtures were 4/5, 6/5, and 12/5. The amounts of phosphate added were 1.3, 2, and 4 times that needed to transform the total soil Pb into pyromorphite based on a 3/5 P/Pb molar ratio in chloropyromorphite [Pb<sub>5</sub>(PO<sub>4</sub>)<sub>3</sub>-Cl].

**Procedures.** The reaction of soil with apatite was conducted in a 1.1-L glass beaker containing a glass pH electrode, a stirring paddle, and an automatic titrator (Toledo, ES 70). The beaker was submerged in a water bath and maintained at a constant temperature of 37 °C. One liter (1.00 L) of 0.1 M NaNO<sub>3</sub> and 0.001 M NaCl solution was adjusted to the desired pH, with 0.1 N HNO<sub>3</sub> and 0.1 N NaOH, prior to adding solid sample. After the soil or soil-apatite mixture was added, the suspension pH was controlled by the autotitrator. In this study, the desired experimental pH was achieved within 30 s after addition of solid and was maintained to ±0.1 of target pH thereafter.

The reported pediatric gastric pH ranges from 1 to 4 and averages 1.7–1.8 in a fasting stomach (12–15). The pH rises to 4–6 following ingestion of food and returns to basal values within 2 h. For an adult, about 80% of stomach emptying occurs during the first hour following ingestion of a meal; a child's stomach empties in 54–68 min, depending upon the type of meal (15). During stomach emptying, the chyme enters the small intestine where the pH rises to 7 and where Pb absorption occurs. Accordingly, the pH range of 2–7 was selected for this study to cover the pH values that occur in the stomach and intestine. In the pH-constant study, the pH in the solution was maintained for 2 h at a constant pH (values from 2 to 7). In the pH-dynamic study, the pH of the solution started at pH 2, was adjusted to pH 7 within 25 or 45 min, and then maintained at pH 7 for 2 h to simulate the pH change that occurs when food is ingested. The selection of pH range and time scale chosen here is based on what may happen in the human stomach. The results obtained from the static system (pH-constant) and the dynamic system (pH-dynamic) can also be applied in other reaction systems, such as soil solutions and waste treatments.

In the pH-constant study, 1.00 g of soil was mixed with the desired amount of apatite and reacted in 1.00 L of solution at pH 2, 3, 4, 5, 6, and 7. After the solid sample was added and pH was stabilized, 5 mL of the suspension was sampled periodically during the following 2 h of reaction. The solution and solid were separated using a 0.2-μm membrane, and the solution was acidified and then analyzed for soluble P, Pb, and Ca concentrations using the inductively coupled plasma spectrophotometer (ICP-AES, Trace 61E, Thermal Jerrel Ash).

In the pH-dynamic study, the solution was initially adjusted and maintained at pH 2 for 3 min after the solid mixture (1.00 g of soil + apatite) was added. The pH was then increased to 7 within 25 or 45 min in two separate experiments, respectively. Two suspension samples were taken at pH values of 2, 3, 4, 5, 6, and 7; the first one was taken 1 min after the desired pH was reached, and the second one was sampled before the suspension was adjusted to the next pH. The concentrations of soluble species (P, Pb and Ca) were quantified with ICP-AES after the suspension was passed through a 0.2-μm membrane.

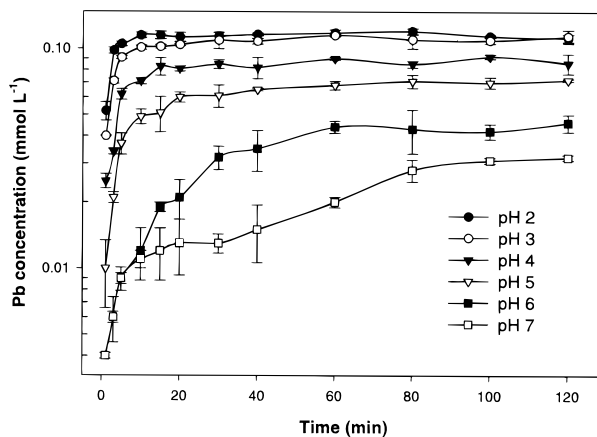


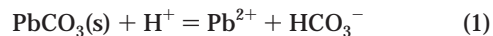
FIGURE 1. Effect of pH on solubility and dissolution rate of soil Pb. Soil concentration = 1.00 g L<sup>-1</sup>.

**Analytical Procedures.** Soluble Ca, P, and Pb concentrations were determined with ICP-AES. The detection limit for the three elements was 2 μg L<sup>-1</sup>. The Water Supply Performance Evaluation Study (WS033, U.S. EPA) solution was used to calibrate the standard solutions. Blanks, standards, and spiked samples were used for analytical quality control.

After the desired reaction period, selected solid samples were collected from both the pH-constant and the pH-dynamic systems for X-ray diffraction analysis. The soil samples were air-dried, passed through a 0.25-mm sieve, and packed on sample holders (30 mm in diameter and 3 mm in depth) for X-ray diffraction analysis. The samples were qualitatively analyzed by the Scintag PADV automated, microprocessor-controlled X-ray powder diffractometer, with Cu Kα X-ray source and Ge solid-state cryogenic detector, operated at 30 mA and 40 kV. Samples were scanned from 20 to 40° 2θ, which covers the characteristic peaks for both cerussite and pyromorphite, using a stepping rate of 0.02° 2θ and scanning rate of 3° per minute.

## Results

**pH-Constant Study.** The soluble Pb in a soil suspension is the result of interactions between Pb-bearing solids and the solution. These interactions include dissolution of lead minerals, dissociation of lead complexes, desorption of adsorbed lead, and the formation of different Pb complexes and solids. Since most of the processes mentioned are pH-dependent, the effect of pH on Pb release from the solids into solution is significant. Soluble Pb concentrations in the soil slurries increase with decreasing pH (Figure 1). As reported elsewhere (8) and confirmed by our own XRD analyses (Figure 5a), the dominant lead mineral in this soil was cerussite, (PbCO<sub>3</sub>), for which the dissolution is a function of pH:



The highest Pb concentration was 0.12 mmol L<sup>-1</sup> at pH 2. This concentration was reached in 3–5 min and remained constant for the 2-h study. Approximately 72% of the total soil Pb was dissolved. The fraction of soil Pb undissolved at pH 2 after 2 h can be considered stable and not bioaccessible soil Pb. This stable fraction of soil Pb may be encapsulated inside soil particles or other insoluble minerals or may exist as Pb mineral released only through total soil digestion with concentrated acid under high temperature. With increasing pH, the saturation concentrations for most lead minerals and the equilibrium concentrations for lead adsorption/desorption and complexation/dissociation decrease. This

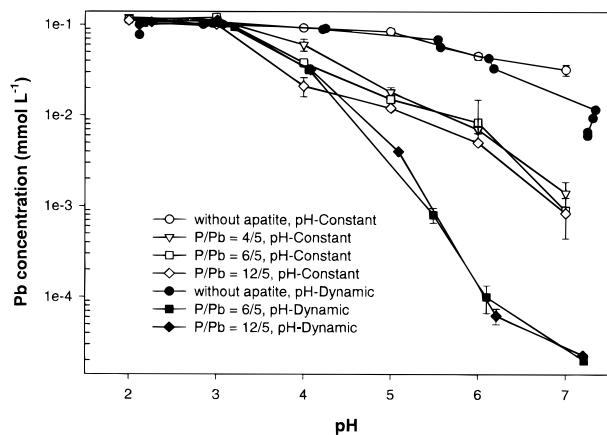


FIGURE 2. Effects of pH on the soluble Pb concentration in the presence of apatite at three P/Pb molar ratios. Reaction time = 120 min, except in the pH-dynamic systems.

generally occurs in an exponential fashion, resulting in a sharp decline in soluble lead concentrations (Figure 1). Furthermore, the time required to reach a steady state increased with pH; and at pH 7, 80–100 min was required. This is consistent with the results obtained from dissolution of pure cerussite (unpublished data).

In addition to dissolution of soil Pb, the dissolution rate of hydroxyapatite is also pH dependent (16, 17). At low pH (pH 2 and 3), the dissolution rate was too rapid to be accurately determined under the experimental conditions used in this study; but as pH increases, the dissolution rate of hydroxyapatite slows dramatically.

Attenuation of soluble Pb in the soil suspensions amended with apatite increased with increasing pH (Figure 2). At pH 2 and pH 3, the differences in soluble Pb between the apatite-treated and nontreated soils were negligible because of the high dissolution rate and solubilities of lead minerals at low pH values; soluble Pb concentrations were  $1.1 \times 10^{-1}$  mM. At pH 4 and above, soluble Pb concentrations decreased in suspensions with or without apatite (Figure 2). Soluble Pb decreased from  $1.1 \times 10^{-1}$  mM at pH 2 to  $3.2 \times 10^{-2}$  mM at pH 7 in the soil suspensions without apatite. In contrast, soluble Pb decreased from  $1.1 \times 10^{-1}$  mM to  $1.2 \times 10^{-3}$  mM at pH 7 in the presence of apatite. Thus, there was a 96% reduction in soluble Pb concentration in the suspensions amended with apatite.

Soluble Pb concentration decreased with increasing amounts of hydroxyapatite added, but the effect was only significant ( $P = 0.05$ ) at pH 4. In contrast, results obtained from cerussite-apatite and anglesite ( $\text{PbSO}_4$ )-apatite reactions (unpublished data) showed that the soluble Pb was inversely proportional to the P/Pb ratio. Generally, greater amounts of apatite provide a greater surface area for reaction, and the rate of phosphate release is greater. This results in faster reduction of soluble Pb. In the soil-apatite system, however, the soluble Ca concentration was rapidly increased by dissolution of soil Ca minerals such as calcite and/or desorption of adsorbed Ca as well as dissolution of apatite to  $2.1 (\pm 0.4)$  mM in the suspensions within 5 min and remained constant for the duration of the experiment. As the solubility product,  $K_{sp}$ , of hydroxyapatite dissolution (eq 2) consists of activities of aqueous calcium, phosphate, and



$$K_{sp} = 10^{15.8(\pm 1.7)} = (\text{Ca}^{2+})^5(\text{H}_2\text{PO}_4^-)^3/(\text{H}^+)^7$$

protons, the Ca released from soil contributes to saturation of the solution with respect to hydroxyapatite, thereby

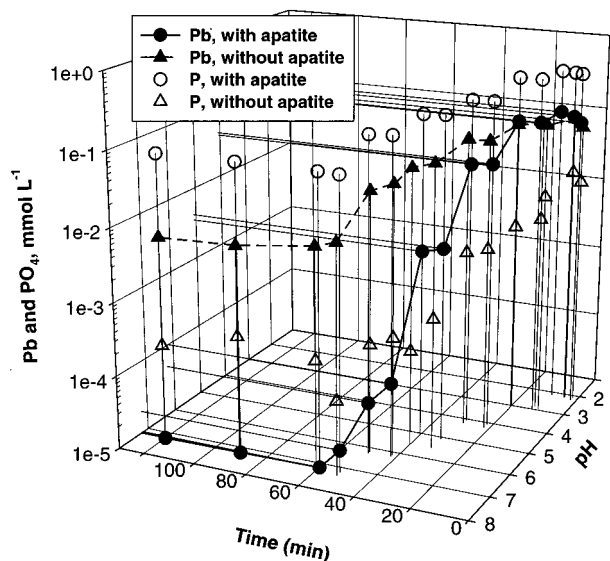


FIGURE 3. Soluble Pb and  $\text{PO}_4$  concentrations in soil suspensions with or without addition of hydroxyapatite (P/Pb = 12/5). The reaction pH was adjusted from 2 to 7 within 45 min.

reducing the amount and rate of phosphate release by hydroxyapatite dissolution. At pH 4 the solution was not saturated with respect to apatite. Soluble Pb decreased proportionally to P/Pb ratio by forming a pyromorphite precipitate (Figure 2). At pH 5 and above, the suspensions were essentially saturated or close to saturation with respect to apatite, even at the low rate of addition. Release of phosphate from apatite dissolution, regardless of the amount of apatite in the suspension, was limited by saturation of the solutions with the soluble Ca from soil calcite dissolution. Consequently, the transformation of Pb from cerussite in the soil to pyromorphite was limited, and the soluble Pb concentration was essentially controlled by the cerussite solubility, regardless of the amount of apatite added.

**pH-Dynamic Study.** To simulate the pH conditions occurring during ingestion, the suspension pH was intentionally adjusted from pH 2 to pH 7 during the first 45 min (7–8 min per pH) of a 2-h reaction. At each pH, two samples were taken: the first, 1 min after the designated pH was reached, and the second, just before the pH was adjusted upward. The similarities in soluble Pb and P concentrations measured at 7–8-min intervals, at each pH, imply that the system reached an apparent steady state rapidly after the pH was adjusted (Figure 3).

Without the addition of apatite, soluble Pb was reduced from  $1.1 \times 10^{-1}$  mM (at pH 2 or 3) to  $9 \times 10^{-2}$  mM (at pH 4.2), to  $7.2 \times 10^{-2}$  mM (at pH 5.5), to  $4.3 \times 10^{-2}$  mM (at pH 6), respectively (Figure 3). These values are in good agreement with those in the pH-constant systems (Figures 1 and 2). The decrease in soluble Pb in the suspension without apatite addition is attributed to adsorption of  $\text{Pb}^{2+}$  onto soil particles. Precipitation of lead minerals, such as lead carbonates and/or lead hydroxide [ $\text{Pb}(\text{OH})_2$ ], can also remove soluble Pb from solution, particularly at high pH values. However, calculations of Pb species distribution in the aqueous phase using the computer code EQ3 (18), and assuming equilibrium failed to show that the solution was saturated with respect to these Pb minerals at these pH values. Furthermore, adsorption of Pb on iron and aluminum oxides and soils increases with pH (19–21). Therefore, it is reasonable to attribute the removal of soluble Pb in the suspension to adsorption and to assume that the soluble Pb level in the suspension was determined by the adsorption/desorption process.



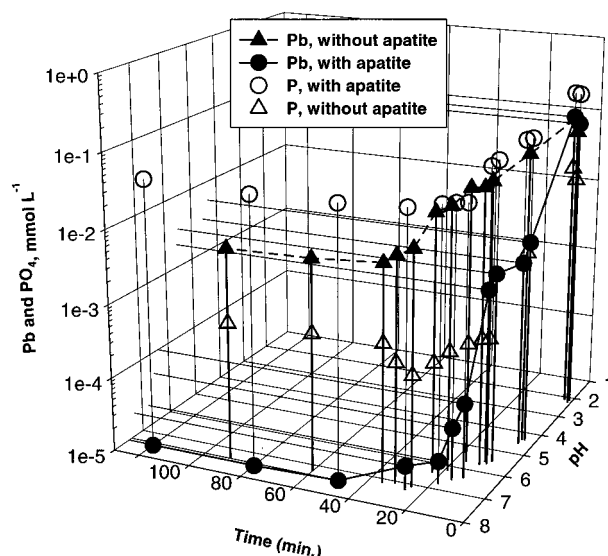


FIGURE 4. Soluble Pb and  $\text{PO}_4$  concentrations in the soil suspensions with or without addition of hydroxyapatite ( $\text{P/Pb} = 6/5$ ). The reaction pH was adjusted from 2 to 7 within 25 min, similar to that found in the gastric condition.

Reactions between soil Pb and added hydroxyapatite in the pH-dynamic system were considerably different from those obtained at constant pH. At low pH (pH 2 and pH 3), soluble Pb did not change regardless of the amount of apatite added (Figure 3). At pH 4, however, the effect of hydroxyapatite addition on soluble Pb levels became apparent; and at pH 5, soluble Pb was more than 1 order of magnitude lower in the presence of apatite than that without apatite (Figure 3). At pH 6, soluble Pb in the suspensions with and without apatite were  $10^{-4.7(\pm 0.2)}$  and  $10^{-1.6}$  mM, respectively, a decrease of more than 3 orders of magnitude. Above pH 6, soluble Pb was at or below the analytical detection limit,  $2 \mu\text{g L}^{-1}$  ( $10^{-5}$  mM), whereas the concentration of soluble Pb remained at the level above  $1 \times 10^{-2}$  mM in the suspension without apatite.

The reduction in soluble Pb in the suspension with apatite was attributed to the formation of chloropyromorphite rather than adsorption/desorption observed in the control. As shown in Figure 3, the soluble  $\text{PO}_4$  was at the level of  $4.2 \times 10^{-1}$  mM, representing the complete dissolution of the added hydroxyapatite. This phosphate level would saturate the solution with respect to chloropyromorphite [ $K_{\text{sp}} = 10^{-18.9(\pm 7.8)}$ , (22)] at pH values  $> 3$ , based on the chloropyromorphite dissolution reaction:



Therefore, precipitation of chloropyromorphite likely occurred as the pH was increased from 3 to 4 and then from 4 to 5. Adsorption of  $\text{Pb}^{2+}$  could happen when pH increased, but Pb adsorbed on soil constituents is transformed into chloropyromorphite if there is a stoichiometric amount of phosphate in the solution (23). In this case, the soluble  $\text{PO}_4$  was maintained at  $10^{-1}$  mM after a pH of 6 was obtained, by which time all of the dissolved lead was converted to chloropyromorphite. The formation of chloropyromorphite in this suspension was confirmed by XRD and will be discussed later.

The effects of rapid pH change (2 to 7 within 25 min) and a lower phosphate application rate ( $\text{P/Pb} = 6/5$ ) on the solubility of soil Pb in the presence of apatite are presented in Figure 4. Added apatite dissolution was complete within 3 min at pH 2.1, and the soluble phosphate concentration

was  $2.4 \times 10^{-1}$  mM (Figure 4). Soluble Pb at this pH was  $1.1 \times 10^{-1}$  mM, similar to that observed in the constant pH experiment (Figure 2) and in the previous dynamic pH experiment (Figure 3). As suspension pH increased to 4.5 and 5.5 (within 5 and 8 min, respectively), soluble Pb decreased to  $2.0 (\pm 0.5) \times 10^{-2}$  and  $2.7 (\pm 0.8) \times 10^{-3}$  mM, respectively. In the system without apatite, soluble Pb concentrations were  $8.2 (\pm 0.4) \times 10^{-2}$  and  $6.1 (\pm 0.5) \times 10^{-2}$  mM at pH 4.4 and pH 5.6, respectively. Thus, within 8 min, soluble Pb was reduced approximately 97% in the presence of apatite, compared with a 45% reduction in the soil without apatite addition. Further increases in pH resulted in greater decreases in soluble Pb concentration and larger differences between the static and dynamic pH systems. Soluble Pb decreased to a level of  $10^{-5}$  mM when the suspension pH reached 7 (Figure 4). In contrast, soluble Pb remained at  $10^{-2}$  mM in the suspension without apatite addition (Figure 4).

In the pH-dynamic system, pH was adjusted from 2 to 7 within 25 or 45 min. As illustrated by comparison of Figures 3 and 4, this change in time had no effect on soluble Pb concentrations or the rate of transformation of soil Pb to chloropyromorphite. Soluble Pb concentrations decreased with increasing pH and were controlled by the solubility of chloropyromorphite. When the pH reached 7, soluble Pb concentrations were essentially equal, at  $2.0\text{--}2.3 \times 10^{-5}$  mM, in the two systems (Figures 3 and 4). This observation illustrates that the formation of chloropyromorphite is rapid and that the soluble Pb concentrations in the pH-dynamic systems are only a function of solution pH.

**X-ray Diffraction Results.** Mineralogical confirmation of chloropyromorphite formation was obtained by X-ray diffraction of selected samples. The original soil mixed with synthetic chloropyromorphite (4% w/w) served as the reference. XRD patterns for this sample indicate that the cerussite was the dominant Pb-bearing mineral in the contaminated soil (Figure 5e). The patterns also show that the soil contains abundant calcite ( $\text{CaCO}_3$ ), which is assumed to reduce the dissolution of the added apatite by saturating the solution with dissolved Ca, as discussed in pH-constant study.

Figure 5, panels a and b, is the XRD patterns for the soils reacted without and with apatite ( $\text{P/Pb} = 12/5$ ) at pH 6 for 60 min. Cerussite was detected in both soil samples, but there was no detectable chloropyromorphite in the apatite-amended soil (Figure 5b). Both soils still had abundant calcite after reaction due to the low dissolution of calcite at pH 6.

Cerussite was completely dissolved in the soils collected from the pH-dynamic systems, as demonstrated in Figure 5, panels c and d, which is the XRD patterns for soil reacted without and with apatite ( $\text{P/Pb} = 12/5$ ), respectively. Calcite was fully dissolved in both soils (Figure 5c,d). Formation of chloropyromorphite was clearly demonstrated in the soil reacted with apatite (Figure 5d). This solid formed as the result of dissolution of cerussite and the precipitation of dissolved Pb reacting with available soluble  $\text{PO}_4$  from apatite dissolution.

Evidence of chloropyromorphite formation was only detected in the soil reacted with apatite in the pH-dynamic suspension (Figure 5d). At the same level of added apatite ( $\text{P/Pb} = 12/5$ ), the formation of pyromorphite was not detected in the soil when pH was uniformly maintained at pH 6 (Figure 5b). These results suggest that in the dynamic pH system (at low pH values such as pH 2 and 3) both cerussite and added apatite were rapidly dissolved. Precipitation of pyromorphite then occurred when the pH was increased. Without reacting for a period at low pH, the dissolution of cerussite and apatite was limited in the pH-constant system,

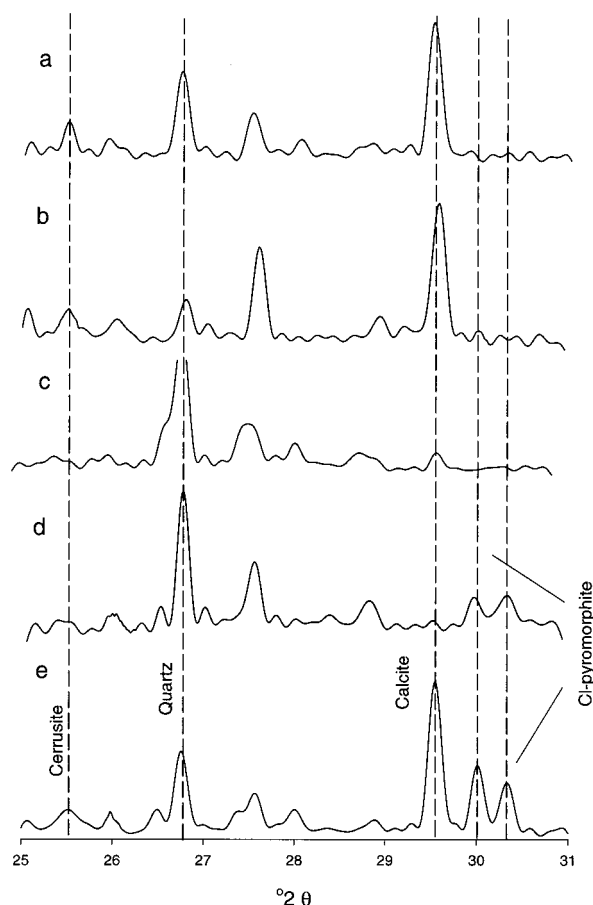


FIGURE 5. XRD patterns for soils reacted without (a) and with (b) apatite at constant pH 6 for 120 min; soils reacted without (c) and with (d) apatite when pH was adjusted from 2 to 7 with 45 min; and the original soil mixed with a synthetic chloropyromorphite, w/w 4% (e).

and there was limited formation of chloropyromorphite. In other experiments of hydroxyapatite reaction with this soil, the effect of pH on pyromorphite formation has been reported (8).

## Discussion

Soil pH is known to affect the soluble Pb concentration, thus the transformation and redistribution of Pb forms is a function of pH. In a dynamic system, such as the GI tract, rapid changes in pH alter reactions and, consequently, may result in solution and mineralogical compositions different from those obtained in constant pH systems, even at comparable pH values. Soluble Pb concentration was lower ( $1.0 \times 10^{-2}$  mM) in a dynamic pH system as compared to a constant pH system ( $3.2 \times 10^{-2}$  mM), when the final pH was pH 7 (Figure 2). The difference was attributed to different mechanisms that govern soluble Pb in the two systems. In the constant pH system, the soluble Pb level is controlled by the solubility of cerrusite, for which dissolution was very limited. By contrast, soluble Pb in the pH-dynamic system was determined by adsorption/desorption processes. At the initial low pH values, cerrusite partially dissolved. As pH increased, adsorption of  $Pb^{2+}$  on soil particle surfaces occurred, and the soluble Pb concentration was reduced. Calculations using the geochemical modeling program EQ3 indicate that no Pb mineral precipitated under these conditions. Therefore, the soluble Pb level was governed by adsorption/desorption of Pb on soil particle surfaces. When the systems were amended with phosphate, the differences

between the soluble Pb levels in the constant and dynamic pH systems were much more pronounced. At pH 5, the difference was 1 order of magnitude and increased to more than 3 orders of magnitude at pH 6 and pH 7 (Figure 2). This can be attributed to a nearly complete dissolution of cerrusite and apatite at the initial low pH in the pH-dynamic system. The high availability of soluble phosphate removed dissolved Pb immediately and formed chloropyromorphite. The newly formed chloropyromorphite then determined the solubility of soil Pb in the dynamic system. In the pH-constant systems, the soil cerrusite, which was only partially dissolved when the  $pH \geq 5$ , determined the solubility of soil Pb. The rate of soluble phosphate released from apatite dissolution was limited and could not rapidly remove all of the dissolved Pb from the aqueous phase at higher pHs (Figure 2).

At  $pH \geq 5$ , the dissolution rates of soil Pb and the added apatite were slow; this resulted in a limited transformation of soil Pb to pyromorphite in the constant pH system. As illustrated by Figure 5b, the soil Pb remained as cerrusite at pH 6 after 120 min reaction; however, as the pH was gradually changed from low (where both soil Pb and apatite had dissolved) to high, the soluble Pb and phosphate precipitated as chloropyromorphite (Figures 3 and 4). Formation of chloropyromorphite in the presence of soluble Pb and phosphate is kinetically and thermodynamically favorable. Thus in the pH-dynamic systems (Figures 3 and 4), the precipitation of pyromorphite was rapid and exclusive. This was confirmed by the XRD analyses (Figure 5d).

In evaluation of the reactivity and/or bioavailability of a Pb-contaminated soil and the effects of remediation efforts by phosphate amendment, the specific conditions under which the Pb-contaminated soil will react have to be considered because they are, as demonstrated in this study, the factors determining the distribution of Pb forms in a specific system. The results from the system with constantly controlled conditions cannot be directly applied to the system in which the reaction conditions behave in a dynamic nature.

## Acknowledgments

This research was supported in part by an appointment to the Postgraduate Research Participation Program at the National Risk Management Research Laboratory administered by the Oak Ridge Institute for Science and Education through an interagency agreement between the U.S. Department of Energy and the U.S. Environmental Protection Agency. Although the research in this paper has been undertaken by the U.S. EPA, it does not necessarily reflect the views of the Agency. Mention of trade names or commercial products does not constitute endorsement or recommendation for use.

## Literature Cited

- (1) Nriagu, J. O. *Geochim. Cosmochim. Acta* **1974**, *38*, 887–898.
- (2) Ma, Q. Y.; Traina, S. J.; Logan, T. J.; Ryan, J. A. *Environ. Sci. Technol.* **1993**, *27*, 1803–1810.
- (3) Xu, Y.; Schwartz, F. W. *J. Contam. Hydrol.* **1994**, *15*, 187–206.
- (4) Chen, X.; Wright, J. V.; Conca, J. L.; Peurrung, L. M. *Environ. Sci. Technol.* **1997**, *31*, 624–631.
- (5) Ma, Q. Y.; Logan, T. J.; Traina, S. J. *Environ. Sci. Technol.* **1995**, *29*, 1118–1126.
- (6) Ruby, M. V.; Davis, A.; Nicholson, A. *Environ. Sci. Technol.* **1994**, *28*, 646–654.
- (7) Cotter-Howells, J. *Environ. Pollut.* **1995**, *90*, 1–8.
- (8) Laperche, V.; Traina, S. J.; Gaddam, P.; Logan, T. J. *Environ. Sci. Technol.* **1996**, *30*, 3321–3326.
- (9) Davis, A.; Ruby, M. V.; Bergstrom, P. D. *Environ. Sci. Technol.* **1992**, *26*, 461–468.
- (10) Ruby, M. V.; Davis, A.; Link, T. E.; Schoof, R.; Chaney, R. L.; Freeman, G. B.; Bergstrom, P. *Environ. Sci. Technol.* **1993**, *27*, 2870–2877.
- (11) Gasser, U. G.; Walker, W. J.; Dahlgren, R. A.; Borch, R. S.; Burau, R. G. *Environ. Sci. Technol.* **1996**, *30*, 761–789.

- (12) Malagelada, J.-R.; Longstreth, G. F.; Summerskill, W. H. J.; Go, V. I. W. *Gastroenterology* **1976**, *70*, 203-210.
- (13) Malagelada, J.-R.; Go, V. L. W.; Sukkerskill, W. H. J. *Dig. Dis. Sci.* **1979**, *24*, 101-110.
- (14) Ruby, M. V.; Davis, A.; Kempton, J. H.; Drxler, J. W.; Bergstrom, P. *Environ. Sci. Technol.* **1992**, *26*, 1242-1248.
- (15) Ruby, M. V.; Schoof, R.; Eberle, S.; Sellstone, C. M. *Environ. Sci. Technol.* **1996**, *30*, 422-430.
- (16) Thomann, J. M.; Voegeland, J. C.; Gramain, P. *Calcif. Tissure Res.* **1990**, *46*, 121-129.
- (17) Christoffersen, J.; Christoffersen, M. R.; Kjaergaard, N. *J. Cryst. Growth* **1978**, *43*, 501-511.
- (18) Wolery, T. J. *EQ3/6, A software pacage for geochemical modeling of aqueous systems*; UCRL-MA-110662; Lawrence Livemore National Laboratory: Livemore, CA, 1992.
- (19) Florence, T. M.; Batley, G. E. *J. Soil Sci.* **1980**, *27*, 154-166.
- (20) Hayes, K. F.; Leckie, J. O. American Chemical Society: Washington, D.C. 1986; pp 114-141.
- (21) Peters, R. W.; Shem, L. *Environ. Prog.* **1992**, *11*, 234-240.
- (22) Nriagu, J. O. *Geochim. Cosmochim. Acta* **1973**, *37*, 367-388.
- (23) Zhang, P.; Ryan, J. A.; Bryndzia, L. T. *Environ. Sci. Technol.* **1997**, *31*, 2673-2678.

*Received for review December 9, 1997. Revised manuscript received June 5, 1998. Accepted June 23, 1998.*

ES971065D